



US 20090180941A1

(19) **United States**

(12) **Patent Application Publication**
Vanderspurt et al.

(10) **Pub. No.: US 2009/0180941 A1**

(43) **Pub. Date: Jul. 16, 2009**

(54) **DEACTIVATION RESISTANT
PHOTOCATALYSTS**

(86) PCT No.: **PCT/US07/12855**

(75) Inventors: **Thomas Henry Vanderspurt**,
Glastonbury, CT (US); **Treese
Hugener-Campbell**, Coventry, CT
(US); **Norberto O. Lemcoff**,
Simsbury, CT (US); **Stephen O.
Hay**, Tolland, CT (US); **Wayde R.
Schmidt**, Pomfret Center, CT (US);
Joseph J. Sangiovanni, West
Suffield, CT (US); **Zissis A.
Dardas**, Worcester, MA (US); **Di
Wei**, Ellington, CT (US)

§ 371 (c)(1),

(2), (4) Date: **Nov. 26, 2008**

Related U.S. Application Data

(60) Provisional application No. 60/809,995, filed on Jun. 1, 2006, provisional application No. 60/810,022, filed on Jun. 1, 2006.

Publication Classification

(51) **Int. Cl.**
B01D 53/38 (2006.01)
B01D 36/02 (2006.01)
B01J 21/06 (2006.01)

Correspondence Address:
KINNEY & LANGE, P.A.
THE KINNEY & LANGE BUILDING, 312
SOUTH THIRD STREET
MINNEAPOLIS, MN 55415-1002 (US)

(52) **U.S. Cl. 423/210; 422/129; 422/120; 502/350;**
502/304; 502/338; 502/343; 502/309; 502/200;
210/749

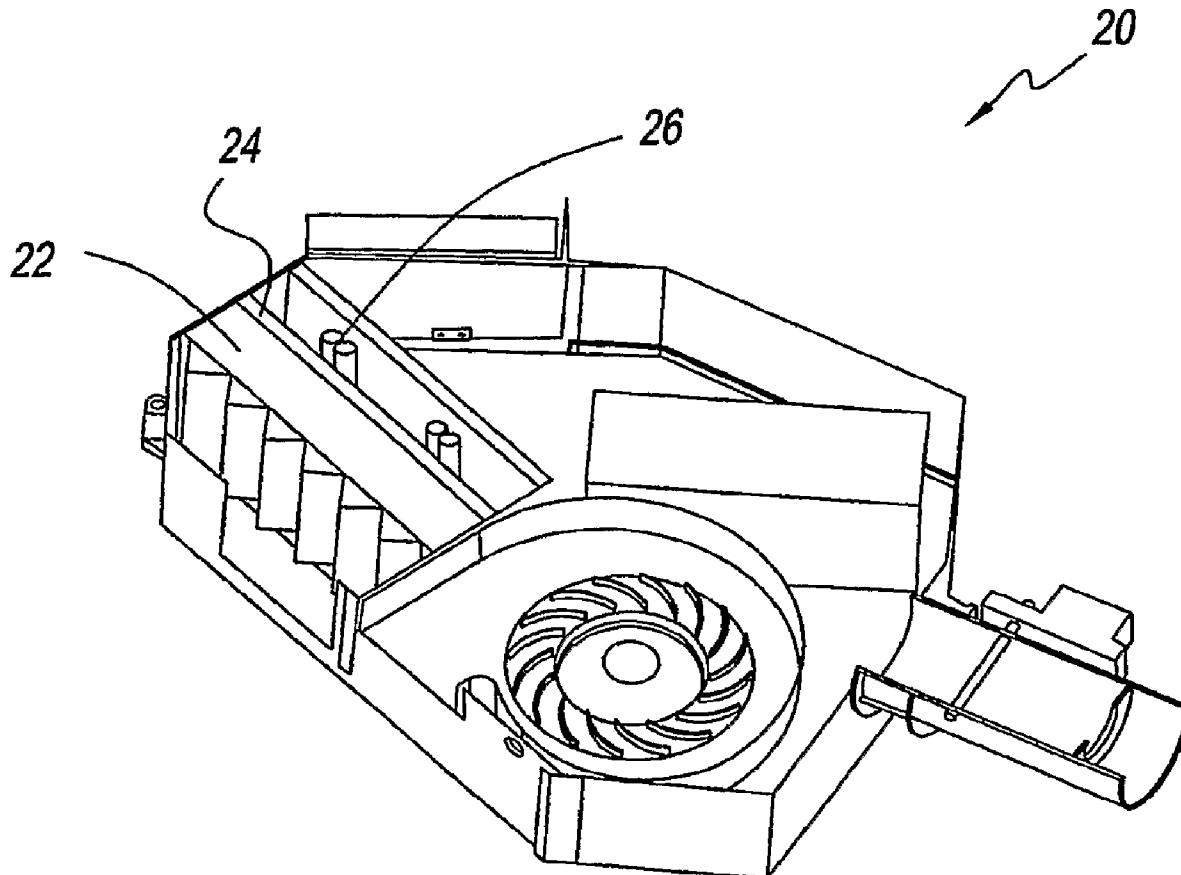
(73) Assignee: **CARRIER CORPORATION**,
Farmington, CT (US)

(57) **ABSTRACT**

(21) Appl. No.: **12/302,626**

The present disclosure relates to a fluid purification device that has a deactivation resistant photocatalyst having nanocrystallites of less than 14 nanometers (nm) in diameter with at least 200 m² surface area/cm³ of skeletal volume in cylindrical pores of 5 nm in diameter or larger, with the mode of the pore size distribution 10 nm or more.

(22) PCT Filed: **May 31, 2007**



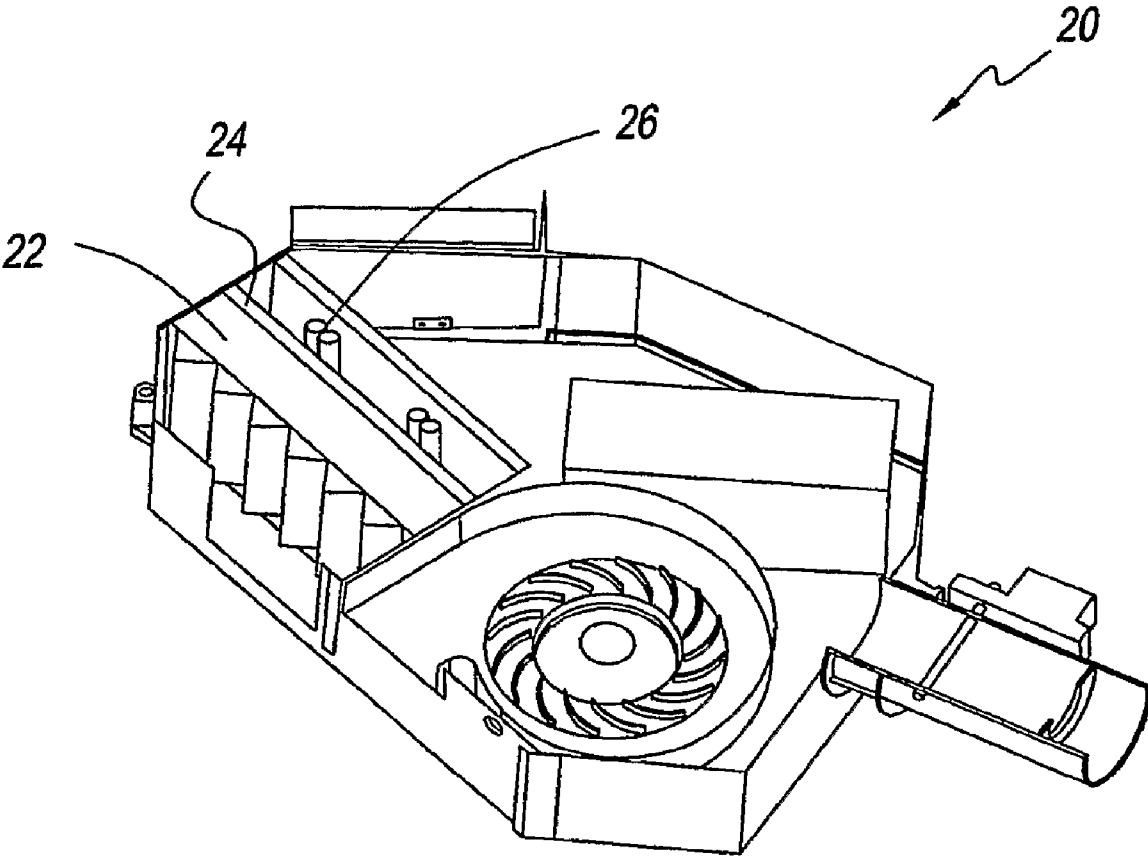


Fig. 1

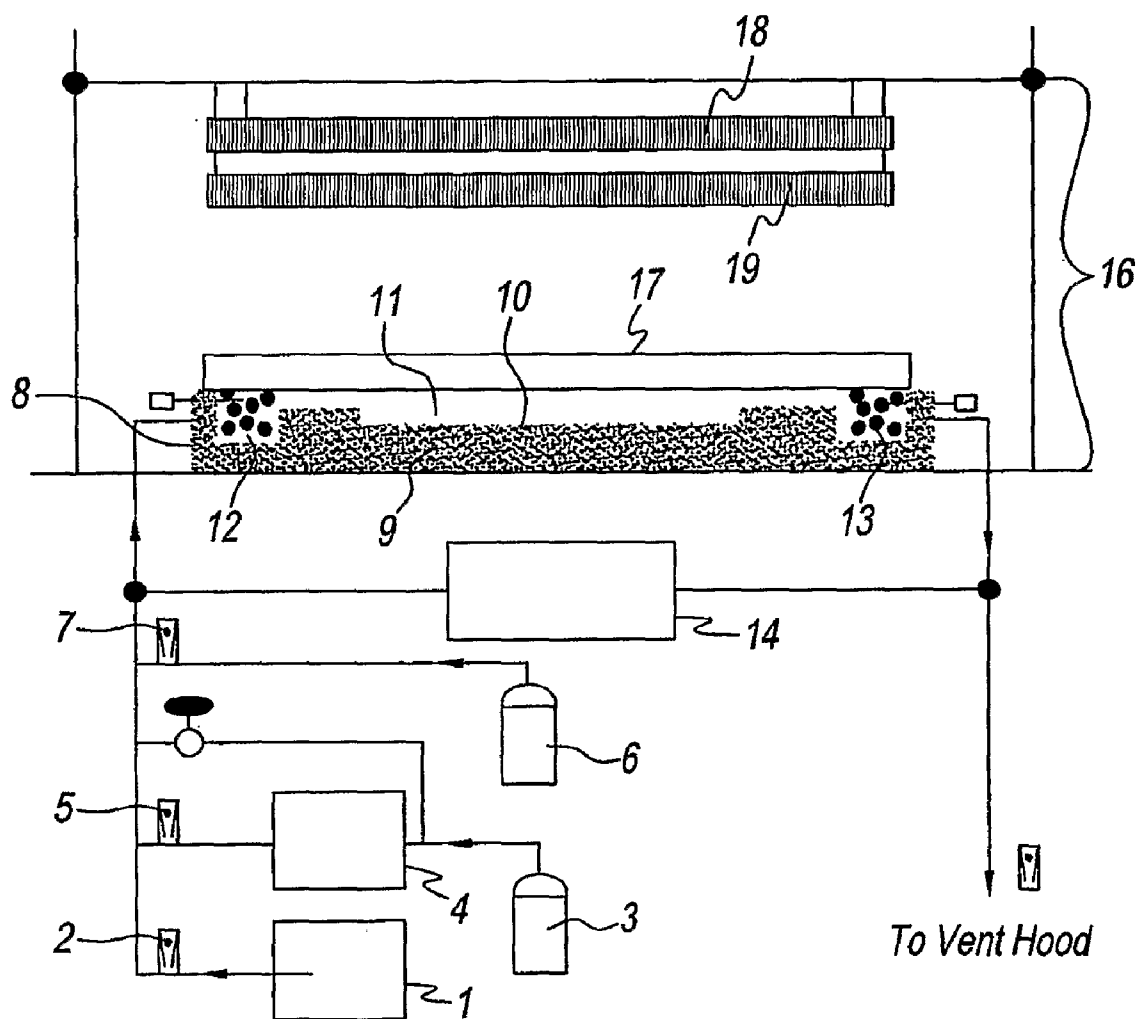


Fig. 2

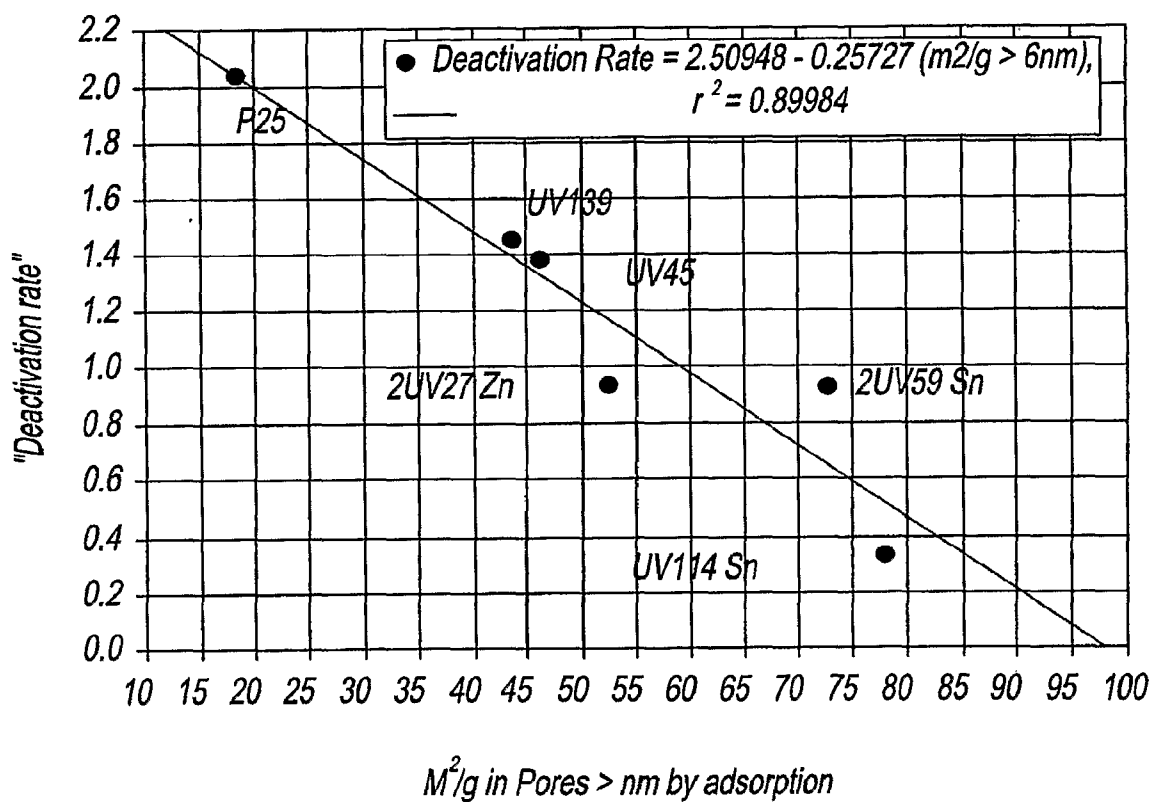


Fig. 3

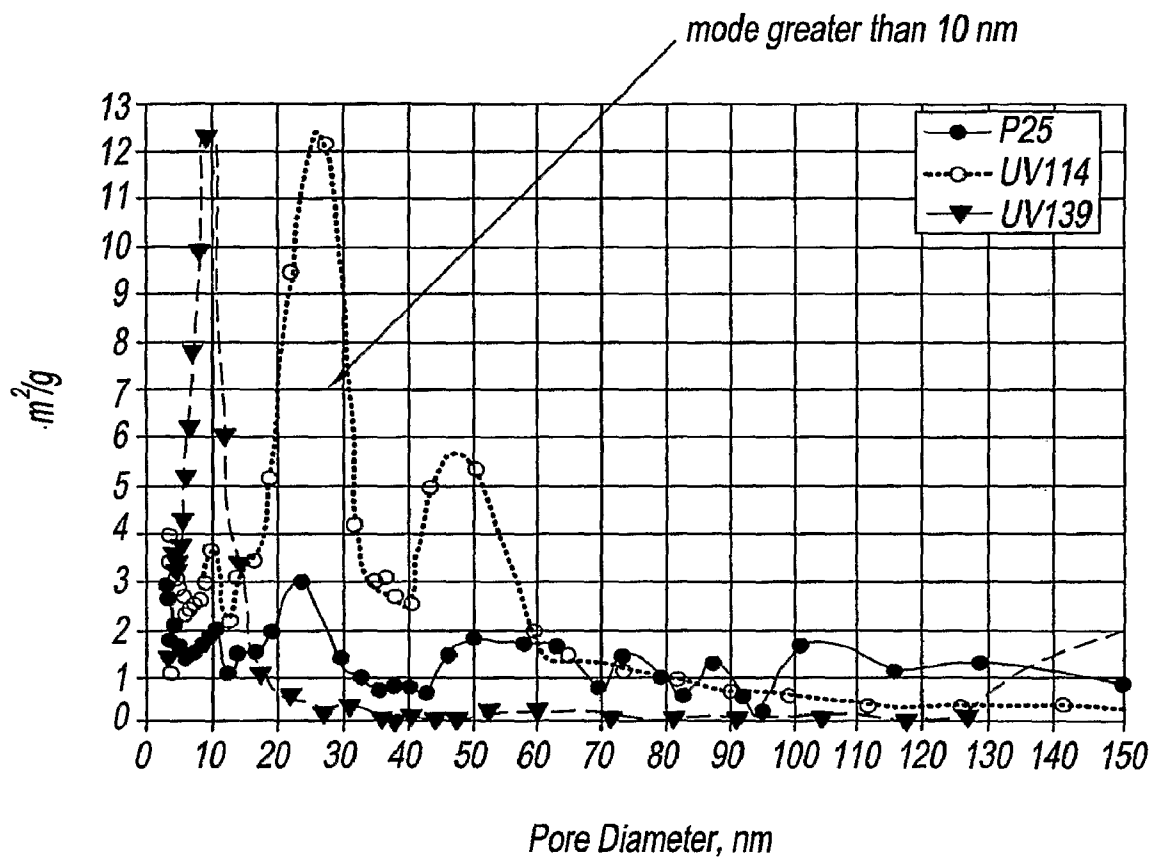


Fig. 4

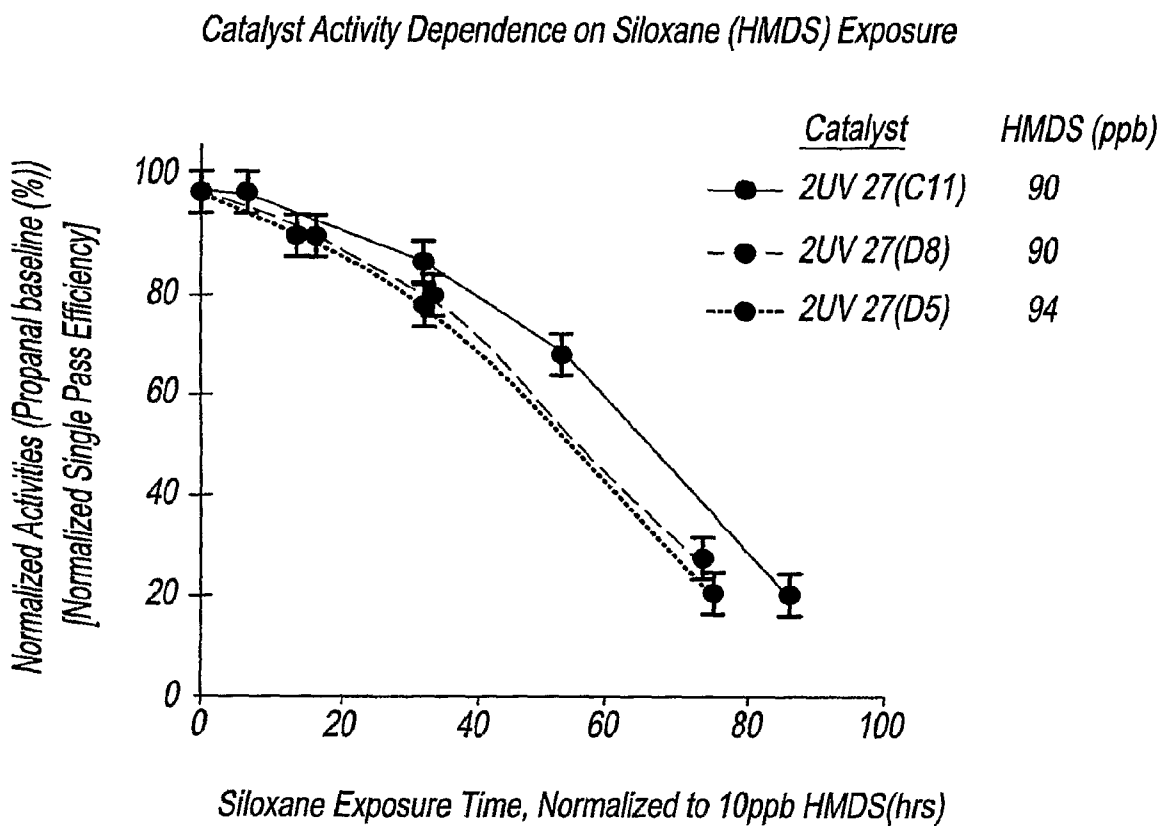


Fig. 5

DEACTIVATION RESISTANT PHOTOCATALYSTS

BACKGROUND OF THE INVENTION

[0001] 1. Field of the Invention

[0002] The present invention relates generally to purification devices having photocatalysts. More specifically, the present invention relates to air purification devices having deactivation resistant photocatalysts.

[0003] 2. Description of the Related Art

[0004] Photocatalytic Oxidation (PCO) is a technology used for elimination or reduction of the level of contaminants in a fluid, like air or water, using the chemical action of light. When ultraviolet (UV) light is used to energize the photocatalyst, the technology is more specifically termed Ultraviolet Photocatalytic Oxidation (UV-PCO).

[0005] Semiconductors have a sufficiently wide band gap energetic enough to activate water or surface hydroxyls thus creating .OH radicals and electrons have been used in purification systems for elimination of organic contaminants. These materials include, but are not limited to, titanium dioxide (TiO₂), zirconium dioxide (ZrO₂), zinc oxide (ZnO), calcium titanate (CaTiO₃), tin (stannic) dioxide (SnO₂), molybdenum trioxide (MoO₃), and the like. Of this group, titanium dioxide (TiO₂) is among the most widely-used of the semiconductor photocatalysts because of its chemical stability, relatively low cost, and an electronic band gap that is suitable for photoactivation by UV light.

[0006] Buildings, vehicles, aircraft, ships and the like may utilize air purification systems to improve the quality of indoor air thus enabling decreased ventilation, create an improved environment, or both. The quality of indoor air is achieved through air purification using either aerosol removal or gaseous contaminant removal technologies. The use of photocatalysis is a proven technology that provides for the removal of gaseous airborne substances such as volatile organic compounds (hereinafter "VOCs") including toluene and formaldehyde from the air supply.

[0007] Photocatalytic air purifiers utilize a substrate or cartridge containing a photocatalyst, usually a titanium oxide based material, that interacts with airborne oxygen and water molecules to form hydroxyl radicals when placed under an appropriate light source, typically an ultraviolet (hereinafter "UV") light source. The hydroxide radicals attack the contaminants thereby initiating oxidation reactions that convert the contaminants into less harmful compounds, such as water and carbon dioxide.

[0008] Titanium dioxide (TiO₂) is the most stable oxide form of the transition metal titanium. TiO₂ is mostly ionic material composed of Ti⁺⁴ cations and O⁻² anions. In powder form, TiO₂ is white and is widely-used in industry to give whiteness to paint, paper, textiles, inks, plastics, toothpaste, and cosmetics. In crystalline form, TiO₂ principally exists as one of three different polymorphic forms: rutile, anatase, and brookite. The two more common polymorphic forms of TiO₂, rutile and anatase, have a tetragonal crystal structure, while the less-common brookite form of TiO₂ has an orthorhombic crystal structure.

[0009] The anatase form of TiO₂, which is a low temperature form, has been reported to have the greatest photocatalytic activity of the three polymorphic forms of TiO₂ when exposed to UV light. This may be due to a wider optical absorption gap and a smaller electron effective mass in the anatase form that leads to higher mobility of the charge car-

riers. Anatase is converted to rutile at temperatures above about 600° C. where it is accompanied by crystallite growth and a significant loss of surface area.

[0010] The rutile and anatase crystalline structures each have six atoms per unit cell. The anatase form is a body-centered structure and its conventional cell contains two unit cells (i.e., 12 atoms). For both the rutile and anatase forms, titanium atoms are arranged in the crystal structure in such a way that neighboring octahedral units share edges and corners with each other. In the anatase structure, four edges of every octahedral unit are shared edges, as compared within the rutile structure, in which two edges of every octahedral unit are shared edges.

[0011] One of the most active of currently-available TiO₂ photocatalysts is Degussa Aeroxide TiO₂ P25 (Degussa Technical Information TI 1243, Titanium Dioxide P25 as Photocatalyst, March, 2002, Degussa Corporation; Business Line AEROSIL, Parsippany, N.J. 07054) consists of about 80% by weight 20 nm anatase TiO₂ crystals and 20% by weight larger, about 40 nm, rutile crystals. On exposure to UV light, electron hole separation can occur. Anatase with a strap gap of 3.20 eV requires higher energy, 385 nm photon, than rutile, 2.95 eV or 420 nm. The hole at the surface takes the form of a hydroxyl radical (.OH) that is a stronger oxidizing agent than ozone or chlorine. The electron on the surface can form active oxygen species through the reduction of dioxygen, perhaps through the formation of superoxide ion, O₂⁻ and then by its further reduction to peroxide dianion, O₂⁻² than can on protonation yield hydrogen peroxide. Hydrogen peroxide is believed to be the principal agent of remote photocatalytic oxidation (PCO), which describes the oxidation of substances that are very close to, but not in direct physical contact with, photoactive TiO₂. The presence of both hydroxyl radicals and an active oxygen species are needed for the effective oxidation of formaldehyde to CO₂ and H₂O over the anatase form of TiO₂. P25 crystallites have an average crystallite size of about 20 nm and a BET surface area of about 50 m²/gram. As used herein, BET, stands for the well known method of Brunauer, Emmett, and Teller, (J.A.C.S. 60 (1938) 309.) surface science to calculate surface areas of solids by physical adsorption of gas molecules. This has been automated to a certain degree by instruments like the Micromeritics® 2010.

[0012] Table 1 provides a comparison of average crystallite size with various measures of surface area, including the anatase and rutile forms of TiO₂.

Average crystallite size, nm	Surface area/skeletal volume, m ² /cm ³	Available surface area m ² /cm ³	Specific surface area, m ² /g anatase	Specific surface area m ² /g rutile
5	1200	800	208	188
6	1000	667	174	156
7	857	571	149	134
8	750	500	130	117
9	667	444	116	104
10	600	400	104	94
11	545	364	95	85
12	500	333	87	78
13	462	308	80	72
14	429	286	74	67
15	400	267	69	63
16	375	250	65	59
17	353	235	61	55

-continued

Average crystallite size, nm	Surface area/skeletal volume, m ² /cm ³	Available surface area, m ² /cm ³	Specific surface area, m ² /g anatase	Specific surface area, m ² /g rutile
18	333	222	58	52
19	316	211	55	49
20	300	200	52	47
21	286	190	50	45
22	273	182	47	43
23	261	174	45	41
24	250	167	43	39
25	240	160	42	38
27	222	148	39	35
29	207	138	36	32
31	194	129	34	30
33	182	121	32	28
35	171	114	30	27
37	162	108	28	25
39	154	103	27	24
40	150	100	26	23

[0013] Deactivation of the photocatalyst limits the effectiveness of photocatalytic air purifiers, and can occur reversibly or irreversibly. As the photocatalysts in air purification systems become deactivated, the systems become less efficient. Maintenance is required in order to clean, repair, and replace equipment. This results in increased operating expenses associated with the air purification systems.

[0014] Accordingly, there is a need for an air purification system containing a photocatalyst that can resist deactivation in general and/or can resist deactivation due to sudden and/or prolonged rises in contaminant concentration.

SUMMARY OF THE INVENTION

[0015] The present disclosure provides a purification device having deactivation resistant photocatalysts and deactivation resistant photocatalysts.

[0016] These and other advantages and benefits of the present disclosure are provided by an air purification device having a porous photocatalyst for removing at least a portion of gaseous volatile organic compounds from an air stream in the presence of light.

[0017] A method of purifying an air stream is also provided. The method includes passing the air stream over a photocatalyst sufficient to oxidize at least a portion of the volatile organic compounds in the air stream.

[0018] The above-described and other advantages and benefits of the present invention will be appreciated and understood by those skilled in the art from the following detailed description, drawings, and appended claims.

BRIEF DESCRIPTION OF THE DRAWINGS

[0019] FIG. 1 is an air treatment device.

[0020] FIG. 2 is an illustration of a laboratory flat plate Intrinsic Rate Reactor (IRR).

[0021] FIG. 3 illustrates the longevity of various TiO₂ based photocatalysts in the presence of 90 ppb hexamethyldisiloxane.

[0022] FIG. 4 illustrates the distribution profile of pore sizes for photocatalysts of the present disclosure as compared with other photocatalysts.

[0023] FIG. 5 illustrates effects of hexamethyldisiloxane concentrations on the deactivation rate of siloxane-resistant catalyst 2UV 27.

DETAILED DESCRIPTION OF THE INVENTION

[0024] It has recently been discovered by the present disclosure that photocatalysts in prior art air purification devices can be deactivated due to the mineralization of silicon compounds, such as siloxanes, on the photocatalysts. It has been determined that the siloxanes arise primarily from the use of certain aerosol-based personal care products, such as hair-spray, or dry cleaning fluids. However, siloxanes can also be generated through the use of room temperature vulcanization (RTV) silicone caulks, adhesives, and the like. When siloxanes are oxidized, non-volatile silicon dioxide or hydrated silicon dioxide is formed, which are believed by the present disclosure to act to deactivate the photocatalyst. Without wishing to be bound by any particular theory, it is believed that the deactivation of photocatalysts by such siloxanes can occur through a number of mechanisms such as, but not limited to, the direct physical blockage of the active sites of the photocatalysts and/or by preventing the VOCs from interacting with the active agent.

[0025] The photocatalyst is titanium dioxide, including suitably doped titanium dioxide TiO₂ supporting about a monolayer of another material like tungsten oxide or nano-sized metal crystallites, as well as zinc oxide, tin oxide or other photocatalytic materials.

[0026] The present disclosure also contemplates the use of photocatalytic mixed metal oxides, an intimate mixture of nano-crystalline photocatalytic oxides and other oxides, such as, but not limited to titanium dioxide, zinc oxide or tin oxide.

[0027] It is known that titania photocatalysts such as Degussa P25 (Deanna C. Hurum, Alexander G. Agrios, and Kimberly A. Gray, J. Phys Chem. B, 107 (2003) 45454549) can be deactivated by certain airborne contaminants that upon oxidation leave a non-volatile deposit on the catalyst surface. Among the most prevalent of these materials are silicon compounds like siloxanes.

[0028] The subject of the present disclosure are photocatalysts rendered deactivation resistant by their porous morphology. Specifically, the photocatalysts have a pore structure with low mass transfer resistance and resists blockage by deposits. This pore structure, preferably comprised of cylindrical pores, having the majority of the surface area with pores that are 5 nm in diameter or larger and at least 200 m² surface area/cm³ of skeletal volume of the aggregate photocatalyst has pores that are 6 nm in diameter or larger. The overall distribution of pore size in the aggregate photocatalyst has a mode of 10 nm or greater, where mode is used to mean the most frequently occurring number or size in a set. This pore structure results in photocatalysts that are resistant to deactivation by environmental contaminants such as siloxane.

[0029] The porosity or pore structure of the photocatalyst can be characterized by its BET (Stephen Brunauer, P. H. Emmett, and Edward Teller, Journal of the American Chemical Society, Vol. 60, 1938, PP 309-319.) surface area, SA, and pore size distribution (PSD). These can be determined using the Micromeritics® ASAP 2010 instrument or its equivalent with its accompanying software packages that included BJH (Barrett, Joyner and Halenda, 1951) analysis for mesopore

adsorption and pore size distribution. It is preferred that a mode of this pore size distribution is 10 nm or larger as illustrated in FIG. 4.

[0030] The photocatalyst of the present disclosure shows that surprisingly the rate of activity loss expressed as % of initial single pass efficiency lost per hour does not decrease with an increase in BET SA as might be expected. Also, the rate of activity loss does not correlate with the surface area in pores smaller than 4 nm. However the rate of activity loss decreases, that is, the life expectancy of the catalyst increases with the SA in pores greater than or about equal to 6 nm in diameter.

[0031] Referring to the drawings, and, in particular, FIG. 1, a simple photocatalytic air purification device, such as the air treatment device having deactivation resistant photocatalyst for removing contaminants from the air is shown. The purification device, **20**, comprises a filter **22**, a photocatalyst **24**, and a UV lamp **26**. Filter **22** removes particulates and optionally has adsorption properties with a preference for siloxanes. The deactivation resistant photocatalyst **24** has crystallites of less than 14 nanometers (nm) in diameter with at least 200 m² surface area/cm³ of skeletal volume in cylindrical pores of 5 nm in diameter or larger, with the mode of the pore size distribution 10 nm or more.

[0032] Referring to FIG. 2, there is provided a laboratory flat plate intrinsic rate reactor **8**. The reactor **8** has a VOC supply **1** and a VOC mass flow controller **2**. The reactor **8** has a nitrogen supply **3** that feeds in to a water bubbler **4**, and then to a moist nitrogen mass flow controller **5**. Reactor **8** also has an oxygen supply **6** and oxygen mass flow controller **7**. Reactor **8** has a machined aluminum block **9**, which has a bed **10** for the catalyst-coated slide **11**. Reactor **8** has glass beads **12**, **13**, that serve to mix and distribute gas. A UV transparent window **17** is positioned above the catalyst coated slide **11** to seal the reactor. The gas atmosphere within the reactor **8** is analyzed by gas analyzer **14**. The reactor has an exit gas flow meter (not shown). Reactor **8** has a first UV-A lamp **18** and a second UV-A lamp **19**. The height of the lamps may be adjusted by the lamp height adjustment **16**.

[0033] Exemplary embodiments of the nanocrystalline TiO₂ having a high surface area and large pore structure according to the present disclosure were tested and compared for deactivation rates to Degussa P25 TiO₂, and the results are provided in Example 1 below.

Example 1

[0034] In this example, the conventional BET-specific surface area measurement units of m²/g are used for convenience. 1" by 3" slides were coated with an aqueous suspension of nanocrystalline TiO₂ and allowed to dry. The TiO₂ coating was sufficient to absorb about 100% of the incident light when used in the intrinsic rate reactor according to FIG. 2. This reactor is a flat plate photocatalytic reactor having UV illumination that is provided by two black-light lamps (SpectroLine XX-15A). The spectral distribution was symmetrical about a peak intensity located at about 352 nm and extended from 300 nm to 400 nm. The illumination intensity was varied by adjusting the distance between the lamp and the titania-coated slide. UV intensity at the reactor surface was measured by a UVA power meter. High-purity nitrogen gas passed through a water bubbler to set the desired humidity level. The contaminants were generated either from a compressed gas cylinder, such as propanal/N₂, or from a temperature controlled bubbler. An oxygen gas flow was then combined with the nitrogen and contaminant flows to produce the desired carrier gas mixture (15% oxygen, 85% nitrogen).

[0035] The titania-coated slides were placed in a well, measuring 1" by 18" that was milled from an aluminum block. The well was then covered by a quartz window that was about 96% UVA transparent. Gaskets between the quartz window and aluminum block created a flow passage above the titania-coated slides. The flow passage had a 1" width and a 2 mm height.

[0036] Contaminated gas entered the reactor by first passing through a bed of glass mixing beads. Next, the gas flow entered a 1" by 2 mm entrance region of sufficient length (3") to produce a fully-developed laminar velocity profile. The gas flow then passed over the surface of the titania-coated slides. Finally, the gas passed through a 1" by 2 mm exit region (3" long) and the second bed of glass beads before exiting the reactor.

[0037] Referring now to FIG. 3, the longevity of various TiO₂ based photocatalysts was determined in the presence of 90 ppb hexamethyldisiloxane, using the intrinsic rate reactor of FIG. 2. The deactivation rate of the photocatalyst was determined by the slope of a straight line that represents the catalyst performance during its initial stages of operation. The value for P25 represents the average of several tests.

[0038] As shown by data in Table 2 below, and as shown graphically in FIG. 3, the rate of photocatalytic activity loss, expressed in % initial activity per hour, decreases as the surface area in pores greater than or about equal to 6 nm becomes larger. However, this linear relationship does not hold with the total BET surface area, or the surface area in pores greater than about 4 nm in diameter, as determined by N₂ adsorption and BJH analysis of this adsorption as performed by a Micrometrics® ASAP 2010 surface area determination unit.

TABLE 2

Catalyst	Rate of activity loss, % initial activity/hr	BET	BET APD	SA ≥ 4 nm	SA ≥ 5 nm	SA ≥ 6 nm
P25	-2.04	52.0	8.8	25.5	20.7	18.5
UV139	-1.45	66.6	8.9	59.2	49.8	43.5
UV45	-1.38	64.6	22.0	50.8	47.6	46.0
2UV27	-0.93	123.1	7.2	101.2	71.7	52.3
2UV59	-0.92	82.5	21.4	76.3	74.5	72.7
UV114	-0.33	99.4	21.4	85.0	80.3	77.8

[0039] Referring now to FIG. 4, the distribution of pore sizes for photocatalysts P25, UV139, and UV114 are shown as the relation of pore diameter, in nm (X-axis) and Specific Surface Area, in m²/g (Y-axis). When the data of Table 2 is considered in light of the pore size distribution data in FIG. 4, the photocatalysts with the lowest deactivation rates not only possess increased surface area in pores of greater than about 6 nm, but also the mode (i.e., most prevalent) pore size is about 10 nm or greater, and may be bimodal, as shown by the graph of pore size for UV114.

[0040] The data in Table 2 shows that UV114, which has about 4.2 times the surface area in pores greater than about 6 nm as compared with P25, has a projected life that is at least 6 times longer than P25 when challenged by hexamethyldisiloxane at a concentration of 90 ppb, under the same UV illumination. Extrapolating these data to a time-averaged concentration of 2 ppb of siloxanes, and assuming that the deactivation rate is linear with respect to concentration of contaminants, UV114 should retain at least 20% of its initial activity after about 10,000 hours, while P25 would be projected to lose about 80% of its initial activity after only about 1,700 hours, under the same challenge of siloxanes. It is

important to note that the catalyst with the highest total BET surface area, 2UV27 does not have the lowest deactivation rate.

[0041] For Example 1, 1 ppm propanal was oxidized by UV-A light at 50% relative humidity, under conditions where about 20% of the propanal was initially oxidized. The deactivation agent was 90 parts per billion (ppb) hexamethyldisiloxane.

[0042] Under these conditions, increasing the pore surface area from about 18.5 m²/g in P25 (by BJH N₂ adsorption) to about 77.8 m²/g in Sn-doped TiO₂ (designated as UV114 of the present disclosure) decreased the rate of deactivation of the photocatalyst from a loss of about 2.05% per hour (for P25) to a loss of about 0.34% per hour for UV114, as compared with their initial photocatalytic activities, respectively,

[0043] Thus, assuming that the photocatalytic deactivation rate is proportional to the siloxane concentration, the activity of P25, in the presence of 90 ppb hexamethyldisiloxane, would be expected to drop to about 50% of its initial activity in about 24 hours. Extrapolating these results to a smaller concentration of the deactivating agent, 1 ppb hexamethyldisiloxane, the photocatalytic activity of P25 would be expected to drop to about 50% of its initial activity in 90 days. By comparison, the photocatalytic activity of UV114 would be expected to drop to about 50% of its initial activity after 550 days in the presence of 1 ppb of hexamethylsiloxane.

EXAMPLE 2

[0044] FIG. 5 illustrates the results of an experiment showing the effect of various hexamethyldisiloxane concentrations on the deactivation rate of a siloxane-resistant catalyst, 2UV27. The abscissa, siloxane exposure time, was normalized to a selected hexamethyldisiloxane level (90 ppb). The linear scaling factor was equal to the exposure time multiplied by the hexamethyldisiloxane concentration divided by 90. Each catalyst was exposed to a controlled level of hexamethyldisiloxane for various periods of time. Periodically, the photocatalytic activity, and hence the rate of deactivation, was determined at various times, using propanal as the probe gas.

[0045] As shown in FIG. 5, the further a data curve trends to the right, the lower the deactivation rate of the photocatalyst. As the rate of deactivation of the photocatalyst decreases, this will correspond to a longer photocatalyst life. As shown by the data curves for 34 ppb hexamethyldisiloxane and 90 ppb hexamethyldisiloxane, the relationship between photocatalyst life and hexamethyldisiloxane concentration is non-linear. A lower concentration of hexamethyldisiloxane thereby results in a progressively longer catalyst life.

[0046] For example, in the particular instance of a deactivation level corresponding to the 50% loss in propanal activity, when the hexamethyldisiloxane level was decreased from 90 ppb to 34 ppb, the photocatalyst life increased by a factor of about 1.2 (ratio of normalized exposure time) over the linear increase corresponding to the ratio of hexamethyldisiloxane concentration (i.e., 2.65 equals 90 divided by 34), for a net increase in life of 3.18 times (i.e., 1.2×2.65). The inference from such data is that lowering the hexamethyldisiloxane concentration, as by using an adsorbent filter, for example, would result in a non-linear increase in photocatalyst life.

[0047] While the present disclosure has been described with reference to one or more exemplary embodiments, it will be understood by those skilled in the art that various changes may be made and equivalents may be substituted for elements thereof without departing from the scope of the present disclosure.

The invention claimed is:

1. A fluid photocatalytic purification device comprising a deactivation resistant photocatalyst for removing contaminants from a fluid.

2. The fluid photocatalytic purification device of claim 1, further comprising a filter.

3. The fluid photocatalytic purification device of claim 1, further comprising an adsorbing filter.

4. The fluid photocatalytic purification device of claim 1, wherein the fluid is air.

5. The fluid photocatalytic purification device of claim 1, wherein the fluid is water.

6. A deactivation resistant photocatalyst comprising a plurality of crystallites of less than 14 nm in diameter with at least 200 m² surface area/cm³ of skeletal volume in pores of 5 nm in diameter or larger, with the mode of the pore size distribution 10 nm or more.

7. The photocatalyst of claim 6, wherein the pores are predominately cylindrical.

8. The photocatalyst of claim 6, wherein the plurality of crystallites are nanocrystallites of TiO₂.

9. The photocatalyst in claim 8, where the TiO₂ is primarily anatase.

10. The photocatalyst of claim 6, wherein the plurality of crystallites are nanocrystallites of TiO₂ and have a plurality of pores with a diameter of at least 5 nm.

11. The photocatalyst of claim 6, wherein the plurality of crystallites are nanocrystallites of TiO₂ that are disposed in aggregates that have at least 200 m² surface area per cm³ of skeletal volume in cylindrical pores of at least 6 nm in diameter.

12. The photocatalyst of claim 6, wherein the plurality of crystallites are nanocrystallites of TiO₂, and wherein the nanocrystallites of TiO₂ comprise a coating or layer of a dopant material selected from the group of metal, metal oxide, non-metal, and any combinations thereof.

13. The photocatalyst of claim 12, wherein the dopant material is combined with the nanocrystallites of TiO₂ in the ratio of Ti_(1-x)M_xO₂ where Ti is titanium, x is a mole percentage and M is the doping material.

14. The photocatalyst of claim 12, wherein the dopant material comprises a metal selected from the group consisting of tin, iron, zinc, cerium, neodymium, niobium, tungsten, and any combinations thereof.

15. The photocatalyst of claim 12, wherein the dopant material comprises a non-metal that is nitrogen.

16. The photocatalyst of claim 12, wherein the nanocrystallites of titanium dioxide are less than 12 nanometers in diameter.

17. The photocatalyst of claim 8, wherein the nanocrystallites of TiO₂ form porous particles of less than 1 micron.

18. A method of using a nanocrystalline TiO₂ photocatalyst to remove contaminants from fluid, water or air, comprising: irradiating the nanocrystalline TiO₂ photocatalyst with UV light; and

contacting contaminants with the TiO₂ photocatalyst,

wherein the nanocrystalline TiO₂ photocatalyst have nanocrystallites that are less than 14 nanometers in diameter.